

Apparatus to visualize flows in superfluid ^4He below 1 K

I. Skachko,^{1,*} J. A. Hay,^{1,†} C. O. Goodwin,^{1,‡} M. J. Doyle,¹ W. Guo,^{2,3} P. M. Walmsley,¹ and A. I. Golov¹

¹*Department of Physics and Astronomy,
The University of Manchester, Manchester M13 9PL, UK*

²*Mechanical Engineering Department,
Florida State University, Tallahassee, FL 32310, USA*

³*National High Magnetic Field Laboratory, Tallahassee, FL 32310, USA*

(Dated: February 26, 2026)

Abstract

We describe a versatile apparatus for optical observations of experimental processes at temperatures down to 0.1 K. The cooling is achieved by a wet cryostat with a ^3He - ^4He dilution refrigerator on a vibrationally-isolated platform, capable of continuous rotation at angular velocity of up to 3 rad s^{-1} . The illumination light beam from lasers on a non-rotating optical table at room temperature is introduced via an optical fiber. The images are transferred to the intensified camera at room temperature through a coherent bundle of 10^5 optical fibers giving a spatial resolution of $\sim 30\ \mu\text{m}$, depending on the magnification used. The adjustment of the position of the illumination light, as well as of the focusing of the camera on the object under investigation, can be controlled remotely with the help of piezoelectric positioners. The apparatus was used for visualization of particles dispersed in superfluid helium at temperatures down to 0.14 K. In one version of experiment, fluorescent light from clouds of excimer molecules He_2^* , generated in liquid helium by electron impact from electrons injected by sharp field-emission tips, was recorded and analyzed. In another, fluorescent particles of diameters between $1\ \mu\text{m}$ and $6\ \mu\text{m}$ were initially loaded onto the horizontal surface of a piezoelectric crystal of LiNbO_3 and then injected into liquid helium by short bursts of high-amplitude oscillations at the crystal's resonant frequency 1 MHz. The particle trajectories were filmed at a frame rate of up to 990 fps and analyzed.

* Present address: UKRI-STFC, Daresbury Laboratory, Warrington WA4 4AD, UK

† Present address: Maxeler Technologies, London W6 0ND, UK

‡ Present address: School of Mathematical Sciences, University of Nottingham, Nottingham NG7 2RD, UK

1. INTRODUCTION

Dynamic tangles of quantized vortex lines in superfluid helium, also known as Quantum Turbulence, are an emerging counterpart of turbulence in classical fluids. While sharing certain common features, such as the Kolmogorov spectrum at larger lengthscales and applicability of the fruitful concept of inertial cascades of energy through lengthscales, they also possess interesting differences associated with the singular nature of the vorticity [1, 2]. The main ingredients of the dynamics of quantum turbulence are reconnections and consequent helical deformations (Kelvin waves) of interacting quantized vortex lines. Theoretical modeling [3] predicts that with decreasing temperature below some 0.5 K, where the viscous damping effectively vanishes, the Kelvin waves become highly underdamped, and new regimes are expected. These include the proliferation of Kelvin waves of all lengthscales including very short ones, the transfer (cascade) of energy towards shorter, dissipative lengthscales via interacting Kelvin waves [4, 5], frequent self-reconnections of vortex lines resulting in the emission of small vortex loops [6, 7], etc.

In previous experiments, certain elementary processes involving discrete vortex lines in superfluid ^4He at temperatures $T \gtrsim 1.4\text{ K}$ have been visualized using suspensions of small tracer particles: counterflowing superfluid and normal components [8, 9], anomalous velocity spectra of particles trapped on vortex lines [10], reconnections of pairs of vortex lines [11], isolated vortex rings [12], driven Kelvin waves on vortex lines [13, 14]. To seek evidence for the novel behavior at lower temperatures, we built an apparatus in which micron-sized particles could be dispersed inside superfluid ^4He at temperatures down to 0.1 K, and their trajectories could be recorded using optical visualization. Doing this at temperatures below 1 K, which requires placing the experimental cell with superfluid helium into the vacuum can of a ^3He - ^4He dilution refrigerator with much limited cooling power, poses several challenges: the impossibility of using the same means of introducing solid tracers into liquid helium as in experiments at higher temperatures (like the injection of gaseous helium-hydrogen mixture [9] or laser ablation of a solid target [13]), limitation on the power of illuminating light and constraints on the types of optical access.

To overcome these challenges, we combined several innovations in a single apparatus (see Fig. 1):

- the experimental cell, filled with superfluid ^4He , with three optical windows was cooled by

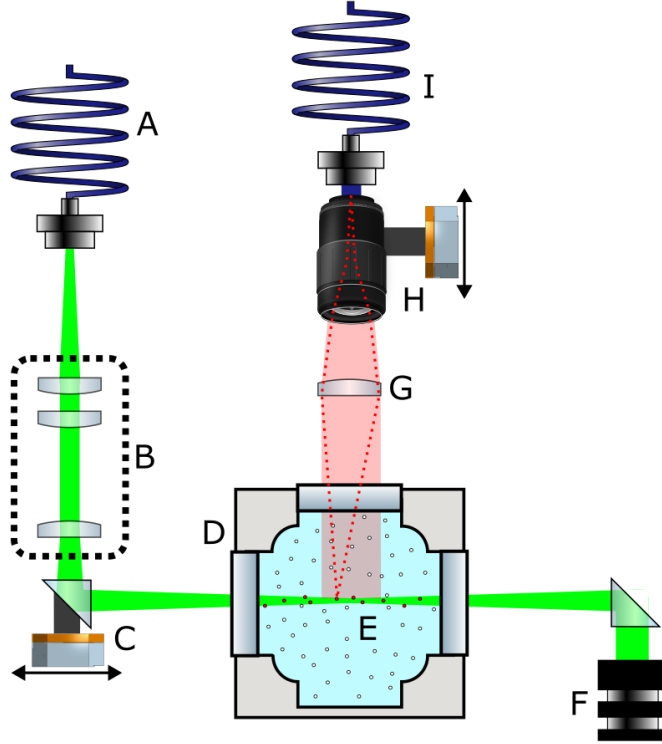


FIG. 1: A schematic of the excitation and imaging optics and the experimental cell. This is the setup used for experiments with excimers and early tests with microspheres: the illuminating light sheet has horizontal profile, and the imaging is through the top window of the cell. In later experiments with microspheres, the light sheet had vertical profile, and the imaging was through a side window. (A) multimode fiber, (B) combination of spherical and cylindrical lenses, (C) movable prism for shifting the light sheet, (D) experimental cell, (E) imaged region inside the cell, (F) dump, (G) achromat lens, (H) movable objective for focusing of the illuminated region onto the fiber bundle, (I) coherent fiber bundle.

- a ^3He - ^4He dilution refrigerator, capable of maintaining temperatures down to 0.1 K;
- the cryostat was placed on a vibrationally-isolated rotating platform while its gas-handling system was placed on another, co-rotating platform [15] – thus allowing us to continuously rotate the experimental cell with superfluid helium and hence, generate and perturb arrays of parallel vortex lines of known density;
- in situ dispersing fluorescent tracer particles of two different types: either He_2^* excimer molecules [16] or micron-size Fluoro-MaxTM polymer microspheres [19];
- high-intensity pulses of light from lasers on a non-rotating laboratory frame were introduced

into the vacuum can of the rotating cryostat using an optical fiber connected through a fiber-optic and electric rotary union [20] and vacuum feedthrough;

- inside the vacuum can, lenses formed the laser light into a light sheet, which illuminated the region of interest inside the experimental cell while passing through it and terminated in the thermally-isolated dump inside the vacuum can;
- the image of the fluorescent particles was focused in situ onto a coherent bundle of 10^5 optical fibers [21] which transferred this image to the intensified camera outside the cryostat;
- both the positioning of the light sheet inside the cell and focusing on it by the camera could be adjusted remotely using piezoelectric nanopositioners [22].

2. EXPERIMENTAL DETAILS

2.1. Experimental cell and cryogenics

The helium cell, made of a ConFlat DN16CF 6-way cube with an inner volume of 13 cm^3 , was thermally linked to the mixing chamber of a customized rotating dilution refrigerator Oxford Kelvinox MX250 [15]. The three antireflection-coated windows, with knife-edge rims, were sealed into DN16CF flanges using copper gaskets. To maximize the transmission of the illuminating light sheet, the corresponding pair of windows was made from either sapphire for the excimer He_2^* excitation at 905 nm or fused silica for the fluorescent particles excited at 532 nm .

The base temperature of the mixing chamber (MC) of the refrigerator before installing the experimental cell and optical components was 12 mK , while currently (whether with the cell empty or full of superfluid helium) it is 61 mK . The cell is suspended from MC on a sequential combination of two copper bars; their substantial total length of ($\sim 30\text{ cm}$) was dictated by the need to accommodate the numerous optical components below the mixing chamber inside the limited space of the vacuum can. The dominant causes of the temperature difference between the cell and MC were likely the thermal resistance of the several compressional connections in the thermal link and the radiation heat load from surrounding optical components at 4.2 K . Currently, the base temperature of the full cell is 139 mK , which is sufficient for experiments in the zero-temperature limit of quantum turbulence ($T \lesssim 300\text{ mK}$), but it can likely be further decreased with future modifications

of the thermal link.

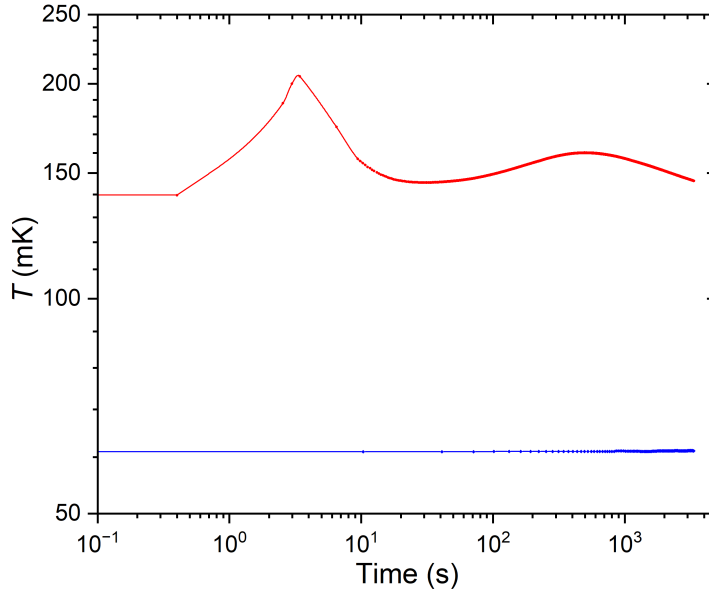


FIG. 2: Temperatures of the cell (top curve, red line and symbols) and of the mixing chamber (bottom curve, blue line and symbols) after firing a $100\ \mu\text{s}$ pulse of 1.0 kV voltage at the piezo transducer at low temperature.

Temperatures were monitored using calibrated resistance thermometers read by two Lake Shore resistance bridges. One bridge was used for slow sequential monitoring of all stages of the refrigerator, while the other was in control of the cell at the highest read-out frequency. An example of the time dependence of the temperatures of experimental cell and MC upon applying a $100\ \mu\text{s}$ -long pulse of 1,000 V voltage to the piezo transducer is shown in Fig. 2. The temperature of MC barely changes while the cell first responds with a temperature surge to slightly above 200 mK within 3–6 s before relaxing towards the initial temperature after $\sim 10\ \text{s}$ – followed by some long-term oscillation of magnitude $\sim 10\ \text{mK}$ on the timescale of an hour, likely caused by a redistribution of temperatures within the refrigerator.

2.2. Optical setup

All major elements of the optical set up are shown in Fig. 3. The beams from lasers on an optical table were combined as necessary and coupled to a multimode optical fiber. The

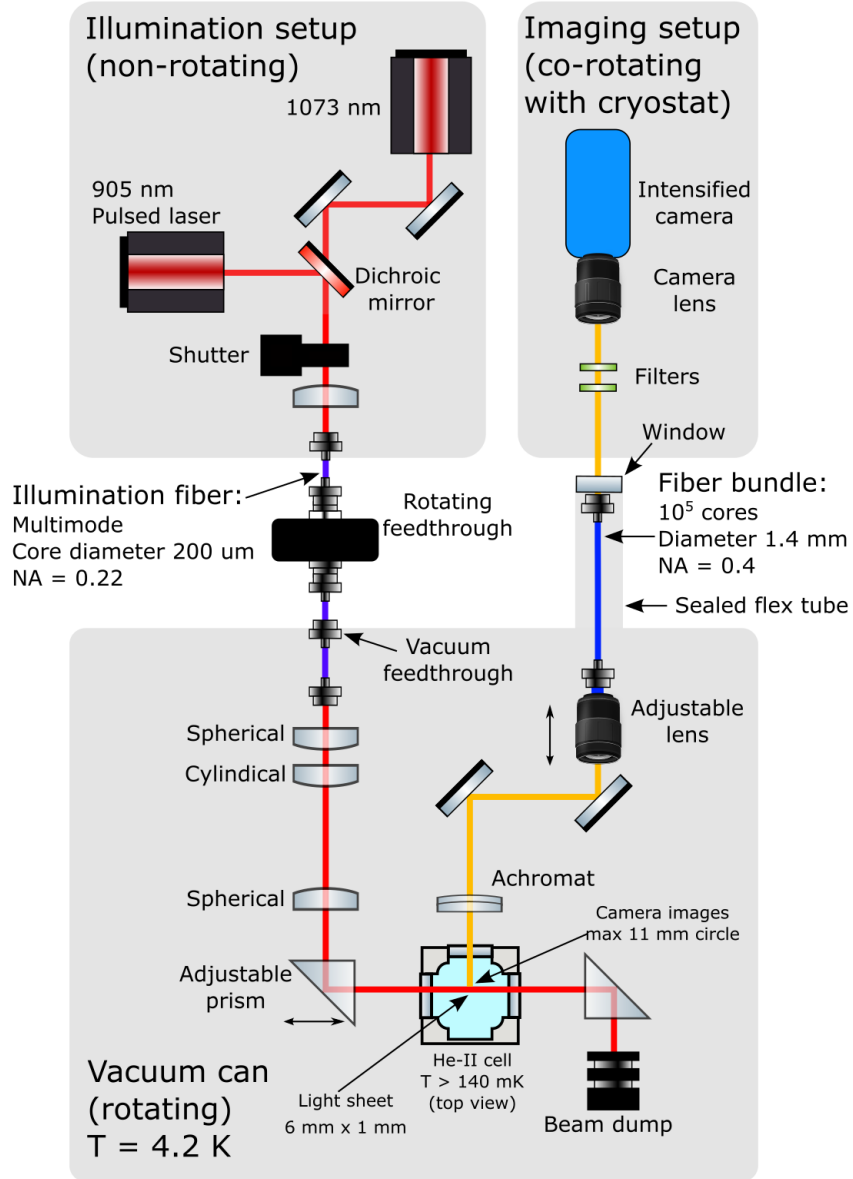


FIG. 3: Elements of the optical set up, grouped by their location by grey rectangles. The two groups at the top are at room temperature outside the cryostat; the left one on a stationary optical table, while the right one is mounted on top of the cryostat. The bottom group is inside the vacuum can of the dilution refrigerator.

latter is fed into the rotating cryostat via a sequence of an optical rotary joint and vacuum feedthrough. Inside the cryostat, the beam exiting the fiber is shaped into an elliptical sheet of either $6 \text{ mm} \times 0.8 \text{ mm}$ (in experiments with He_2^* excimers) or $11 \text{ mm} \times 1 \text{ mm}$ (with

microspheres) using an anamorphic system consisting of one cylindrical and two spherical antireflection coated N-BK7 lenses – before entering the cell with superfluid ^4He . After crossing the cell, the beam is diverted into the beam dump, thermally anchored to the helium bath of the cryostat at 4.2 K. The location of the light sheet inside the cell and focusing of the imaging lens could be adjusted remotely with the help of prisms mounted on piezo translation stages [22]. All optical components inside the vacuum can were anchored to the 4.2 K stage.

The light from fluorescence emerging from the cell is focused, after passing through a sapphire window, on the coherent fiber bundle [21] using a system of lenses. To minimize aberrations and maximize light collection by the fiber bundle with its numerical aperture NA whilst maintaining the desired spatial resolution, a four lens imaging system was designed. In a typical experiment we imaged an illuminated layer of liquid of between ~ 6 mm and ~ 11 mm in diameter onto the face of the fiber bundle of diameter 1.4 mm. The required magnification is hence between $M \approx 0.25$ and $M \approx 0.13$. The ambient temperature end of the fiber bundle is placed in close proximity to the sealed window from the vacuum can, facing the camera at the top of the cryostat. The emerging image is then focused onto the sensing element of the camera.

With a magnification of $M = 0.13$, the diffraction blur at the receiving end of the coherent fiber bundle is only $\sim M \times \frac{1.22\lambda}{D}L = 0.5 \mu\text{m}$ (here the wavelength is $\lambda = 640$ nm, the achromat lens’s diameter and distance from the illuminated region are $D = 25$ mm and the $L = 130$ mm, respectively). The actual resolution of the size of particles was set by the diameter of individual fibers of $4.2 \mu\text{m}$. Further broadening of particle images would stem from occasional overlap of the particle’s image on neighboring fibers as well as from the optical cross-talk between neighboring fibers. Hence, the conservative lower limit of $4.2 \mu\text{m}$ corresponds to the actual diameter inside the cell of $4.2 \mu\text{m}/M = 32 \mu\text{m}$. At the camera end of the bundle of 10^5 fiber cores when projected onto the camera’s matrix area with 1000×1000 pixels, each core is imaged by at least 3 pixels across. The bottom line is that the size of particles of diameter smaller than $\sim 30 \mu\text{m}$ could not be resolved; they would all appear as bright spots of diameter of at least ~ 3 pixels, and only their brightness could be used as a proxy of the particle’s size.

The pulsed laser unit was EKSPLA 252NT, allowing generation of 3–6 ns long pulses with wavelength tunable in the range 670–2600 nm, the maximum pulse energy of 2 mJ and

pulse repetition rate of 1 kHz. This provides a sufficient power density for reaching the He_2^* saturation intensity [16] of 2.2 mJ cm^{-2} . To speed-up the relaxation of excited vibration states of He_2^* to the ground state, an auxiliary continuous 1073 nm laser beam of intensity 3 W cm^{-2} was added. When using fluorescent microspheres as tracers, only pulsed light of wavelength 532 nm was used for illumination.

The camera PCO dicam C1 had an intensifier coupled to an sCMOS sensor with 2048×2048 pixels and a full frame rate of 200 fps. The initial photocathode has quantum efficiency QE of 45% at 640 nm, so around half of all incoming photons were detected. The minimum gating time is 4 ns which is well below the ~ 100 ns radiative lifetime of the He_2^* [16]. The GaAsP photocathode has a diameter of 25 mm requiring a magnification of circa 18 when imaging the fiber bundle. With 100 exposures of 200 ns per frame we expected only around one dark electron per frame. Videos were recorded at 200, 415 or 990 fps with images of 1001×1000 , 500×1000 and 200×1000 pixels, respectively.

2.3. Types of particles

We experimented with two types of tracer particles in liquid helium:

- (i) He_2^* excimers [16] in the triplet state with a lifetime of 13 s – which can be excited by sequential absorption of two photons of wavelength 905 nm followed by spontaneous emission (fluorescence) at 640 nm. Thanks to their considerable effective radius of 0.6 nm one would expect them to stay trapped on vortex lines at temperatures below $\sim 0.6 \text{ K}$ [23] with the trapping diameter of $\sim 100 \text{ nm}$, although the trapped lifetime could be severely shortened by their collisions with other trapped He_2^* molecules and ^3He impurities. He_2^* can be created by an electron impact. Our main interest in using them as vortex tags was in that they are atomically small (i. e. the least invasive), can be created in situ and then disappear without leaving contamination, and are also electrically neutral (unlike positive and negative ions of comparable size, which are frequently used to manipulate and detect the presence of vortex lines [17, 18]).
- (ii) Solid particles of diameter 1–6 μm made from a fluorescent polymer (microspheres) [19], which can be excited by the light of a convenient wavelength 532 nm and then emit photons at circa 640 nm. These particles are relatively large and not neutrally buoyant; yet they can still yield information about the structure and dynamics of the turbulence in

both normal and superfluid components. Thanks to the substantial binding energy, they are expected to be trapped by vortex lines, although their large mass and strong interaction with thermal excitations (‘the normal component’) of superfluid helium might cause intermittent liberation [24].

3. EXCIMERS

The excimers were produced by electron impact from electrons injected into helium from a sharp tungsten tip [25] at voltage ~ 500 V. There were two tips mounted on opposing flanges at right angles to both the excitation and fluorescence beam. Each could be used to generate a vortex tangle and produce excimers [23]. Each tip had two 97.3% transparency tungsten meshes mounted in front of them separated by 1 mm. The closest grid to the tip was an independent electrode whilst the farther grid was grounded to the cell body.

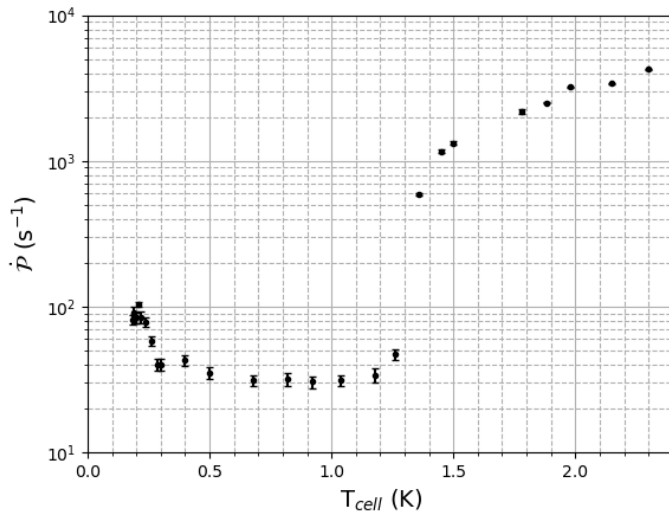


FIG. 4: Received photon flux vs. temperature for excimers generated by pulses of electron currents of order 1 nA for 0.2 seconds.

Tracing individual excimers requires receiving and recording, within the limited NA of our telescope, quantum efficiency of the camera and background noise, of photons from the same molecule in each consecutive video frame (which might be possible in principle but only for long exposures with some 1000 excitation-emission cycles per frame). Instead, in our experiments, we measured the total number of photons from excimers, recorded by the

camera from the given solid angle and imaged area in the given time, which is shown versus temperature in Fig. 4.

At the temperatures at which excimers are expected to be permanently bound to vortex lines, $T \lesssim 0.6$ K, they move ballistically through helium, and the cross-section for trapping on vortex lines is small. Furthermore, even if trapped, their lifetime becomes greatly shortened by the presence of other trapped excimers and ^3He atoms, which concentrate at the cores of quantum vortices at low temperatures. We did use very pure ^4He from Peter McClintock's laboratory in Lancaster with the apparent ^3He concentration of somewhere between 2×10^{-10} – 2×10^{-15} (not precisely known [26–28]). Unfortunately, no detectable densities of excimers, trapped on vortex lines, have been observed in our experiments at any temperatures down to 0.2 K.

At temperatures $T \gtrsim 1.3$ K, when excimers are entrained by the viscous normal component, we routinely recorded time-dependent profiles of fluorescent light from their clouds. The propagation of the front of a turbulent jet of the coupled normal and superfluid components, propelled by the momentum from electrons injected by the field-emission tip, was thus investigated. These results, along with the absorption spectra of He_2^* in liquid helium down to 0.2 K, will be published elsewhere.

4. SOLID PARTICLES

Having little luck with excimers as vortex markers, we turned to solid particles dispersed in situ. These were dyed polystyrene spheres (Fluoro-Max [19]), of radius $a = 2.9 \mu\text{m}$ and density $\rho_p = 1.055 \text{ g cm}^{-3}$. As they are not neutrally buoyant, the particles are constantly under the vertical force $F_g = \frac{4\pi}{3}a^3(\rho_p - \rho_{\text{He}})g$, where $\rho_{\text{He}} = 0.145 \text{ g cm}^{-3}$ is the density of liquid helium and g is the gravitational field strength.

To disperse particles, a disk (12.7 mm diameter, 1 mm thickness) of a piezoelectric crystal 36° Y-cut LiNbO_3 [29] with resonance at 1 MHz of $Q = 500$ (when in liquid ^4He) at the bottom of the cell was initially covered with many layers of dry particles. These could be jettisoned into liquid helium by applying a short (100 μs) burst of AC voltage of frequency 1 MHz and amplitude 0.8–1.5 kV. This method of dispersing particles in superfluid helium [30] was pioneered in the group of Humphrey Maris following their extensive research on the use of piezo transducers in liquid helium. Unlike the method [31] utilizing vibrations from

a room-temperature ultrasonic vibrator, suitable for helium-bath cryostats at temperatures ~ 2 K, high-Q piezo transducers allow application of large-amplitude vibrations inside a ^3He - ^4He dilution refrigerator at temperatures down to 0.1 K and lower.

Compared to excimers, these particles are much brighter even though they require much lower light intensities for the excitation of fluorescence. For illumination, we used laser light of wavelength 532 nm and power ~ 100 mW, since with higher intensities a temperature gradient in the cell would induce a current of the normal component (counterflow), which in turn caused a horizontal drift of particles towards the exit window.

To automatically track trajectories of particles (Particle Tracking Velocimetry, PTV), an algorithm was developed which detects the centers of bright spots in the images and links them from frame to frame – along with several methods of protection from the background noise and erroneous linking. This algorithm, along with the detailed analysis of the different types of trajectories listed below, will be described in forthcoming publications.

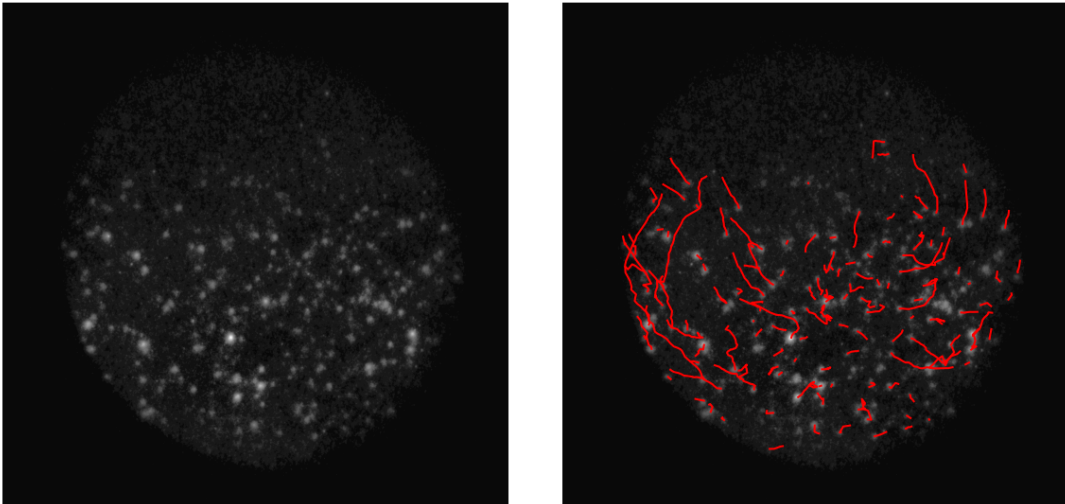


FIG. 5: An image of particles taken at 200 fps (left panel), along with superimposed particle trajectories in red (right panel), $T = 0.8$ K.

We were able to disperse particles at all temperatures between 0.2 K and 1.2 K. During about 1 s following the injection large-scale turbulent eddies were evident. At later times they decayed, and simple settling of particles could be monitored. However, in both regimes, certain particles did not follow similar smooth trajectories of the majority of their neighbors but moved either with different velocity and direction or had quite erratic trajectories. We

associate this behavior with the particles being trapped on vortex lines. Also, there were cases of very bright particles, which we associate with clumps of several particles – these were usually moving slowly and often erratically, most likely being trapped by one or more vortex lines. In Fig. 5, an example is shown of an image taken at $T = 0.8$ K (left), along with superimposed particle trajectories (right).

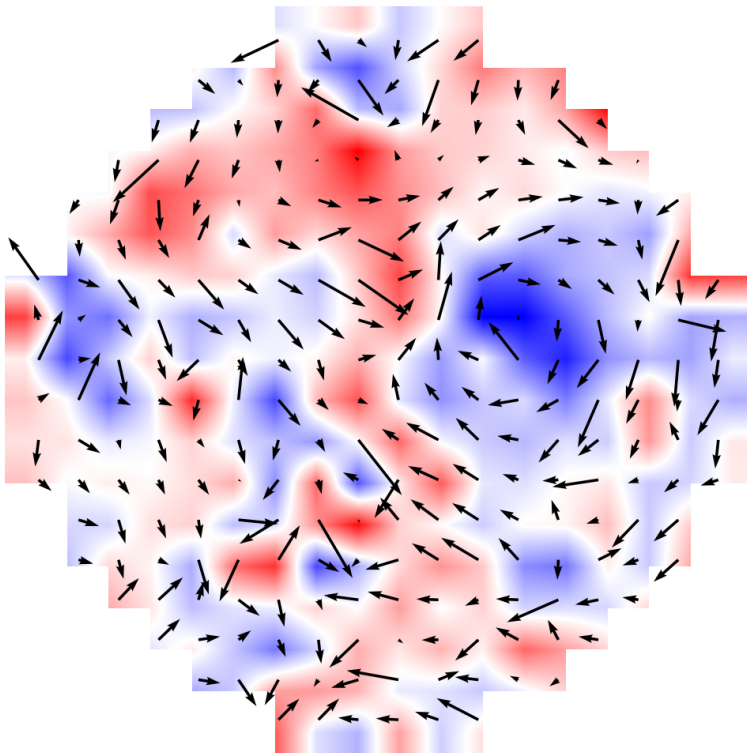


FIG. 6: Map of the particle velocity with corresponding vorticity, $T = 1.0$ K.

At temperatures $T > 0.8$ K, at which the normal component is expected to behave hydrodynamically, swirling motion of particles has been observed. An example of a map of the mean velocity field (Particle Image Velocimetry, PIV) is shown in Fig. 6.

5. CONCLUSIONS

An apparatus was constructed, capable of taking photos of the light emitted by small fluorescent particles dispersed in superfluid ^4He at temperatures down to 0.2 K, also in rotation. The images of an area of dimensions $2.3 \text{ mm} \times 11 \text{ mm}$ can be taken at up to 990 frames per second with the spatial resolution of particle's positions of $\sim 30 \mu\text{m}$.

With excimer molecules He_2^* , only the cumulative brightness of the emitted light and not the positions of individual molecules could be recorded. The analysis of the absorption spectroscopy of He_2^* at temperatures down to 0.2 K and of the dynamics of the propagation of a jet of the normal component, decorated by He_2^* , at temperatures near 1 K will be published elsewhere.

With micron-sized polymer particles, clear trajectories of particles could be recorded, which then allowed their analysis in terms of either PIV or PTV to be applied. The analysis of the tracks of these particles, trapped by vortex lines or free, at temperatures 0.2 K–1.2 K is ongoing.

ACKNOWLEDGMENTS

This work was largely inspired by our collaboration with Joe Vinen, who was eager to understand the dynamics of tangles of vortex lines in superfluid helium in the zero-temperature limit. The financial support came from EPSRC through grant No. EP/P025625/1. W. Guo acknowledges support from the Gordon and Betty Moore Foundation through Grant DOI 10.37807/gbmf11567 and the National High Magnetic Field Laboratory at Florida State University, which is supported by the National Science Foundation Cooperative Agreement No. DMR-2128556 and the State of Florida. Data supporting this study are included within the article and supporting materials.

AUTHOR DECLARATION

The authors have no conflicts to disclose.

DATA AVAILABILITY

The data that support the findings of this study are available within the article.

[1] W. F. Vinen and J. J. Niemela, “Quantum Turbulence”, *J. Low Temp. Phys.* **128**, 167 (2002).

- [2] C. F. Barenghi, L. Skrbek, K. R. Sreenivasan, “Quantum Turbulence”, Cambridge University Press (2023).
- [3] M. Tsubota, T. Araki and S. K. Nemirovskii, “Dynamics of vortex tangle without mutual friction in superfluid ^4He ”, Phys. Rev. B **62**, 11751 (2000).
- [4] B. V. Svistunov, “Superfluid turbulence in the low-temperature limit”, Phys. Rev. B **52** 3647 (1995).
- [5] W. F. Vinen, “Kelvin-Wave Cascade on a Vortex in Superfluid ^4He at a Very Low Temperature”, Phys. Rev. Lett. **91**, 135301 (2003).
- [6] Evgeny Kozik and Boris Svistunov, “Kolmogorov and Kelvin-wave cascades of superfluid turbulence at $T = 0$: What lies between”, Phys. Rev. B **77**, 060502(R) (2008).
- [7] J. Laurie and A. W. Baggaley, “A note on the propagation of quantized vortex rings through a quantum turbulence tangle: Energy transport or energy dissipation?”, J. Low Temp. Phys. **180**, 95 (2015).
- [8] T. Zhang, S. W. Van Sciver, “The motion of micron-sized particles in He II counterflow as observed by the PIV technique”, J. Low Temp. Phys. **138**, 865 (2005).
- [9] G. P. Bewley, D. P. Lathrop, K. R. Sreenivasan, “Superfluid helium - Visualization of quantized vortices”, Nature, **441**, 588 (2006).
- [10] M. S. Paoletti, Michael E. Fisher, K. R. Sreenivasan, and D. P. Lathrop, “Velocity Statistics Distinguish Quantum Turbulence from Classical Turbulence”, Phys. Rev. Lett. **101**, 154501 (2008).
- [11] G. P. Bewley, M. S. Paoletti, K. R. Sreenivasan, and D. P. Lathrop, “Characterization of reconnecting vortices in superfluid helium”, PNAS **105**, 13707 (2008).
- [12] Y. Tang, W. Guo, H. Kobayashi, S. Yui, M. Tsubota & T. Kanai , “Imaging quantized vortex rings in superfluid helium to evaluate quantum dissipation”, Nat. Commun. **14**, 2941 (2023).
- [13] Y. Minowa, Y. Yasui, T. Nakagawa, S. Inui, M. Tsubota and M. Ashida, “Direct excitation of Kelvin waves on quantized vortices”, Nature Physics **21**, 233 (2025).
- [14] C. Peretti , J. Vessaire, É. Durozoy, and M. Gibert, “Direct visualization of the quantum vortex lattice structure, oscillations, and destabilization in rotating ^4He ”, Sci. Adv. **9**, eadh2899 (2023).
- [15] M. J. Fear, P. M. Walmsley, D. A. Chorlton, D. E. Zmeev, S. J. Gillott, M. C. Sellers, P. P. Richardson, H. Agrawal, G. Batey, and A. I. Golov, “A compact rotating dilution refrigerator”,

- Rev. Sci. Instr. **84**, 103905 (2013).
- [16] W. G. Rellergert, S. B. Cahn, A. Garvan, J. C. Hanson, W. H. Lippincott, J. A. Nikkel, and D. N. McKinsey, “Detection and Imaging of He_2^* Molecules in Superfluid Helium”, Phys. Rev. Lett. **100**, 025301 (2008).
- [17] A. Phillips and P. V. E. McClintock, “Field emission and field ionization in liquid ^4He ”, Phil. Trans. A **278**, 271 (1975).
- [18] P. M. Walmsley and A. I. Golov, “Coexistence of Quantum and Classical Flows in Quantum Turbulence in the $T = 0$ Limit”, Phys. Rev. Lett. **118**, 134501 (2017).
- [19] Fluoro-MaxTM fluorescent microspheres
- [20] Doric Lenses, <https://www.doriclenses.com/>
- [21] Fujikura FIGH-100-1500N optical fiber bundle with 10^5 cores, numerical aperture 0.4, image circle diameter 1.4 mm and inter-core separation of $\approx 4 \mu\text{m}$.
- [22] Attocube, <https://www.attocube.com/en/products/nanopositioners>
- [23] D. E. Zmeev, F. Pakpour, P. M. Walmsley, A. I. Golov, W. Guo, D. N. McKinsey, G. G. Ihas, P. V. E. McClintock, S. N. Fisher, and W. F. Vinen, “Excimers He_2^* as Tracers of Quantum Turbulence in ^4He in the $T = 0$ Limit”, Phys. Rev. Lett. **110**, 175303 (2013).
- [24] D. Kivotides, Y. A. Sergeev, and C. F. Barenghi, “Dynamics of solid particles in a tangle of superfluid vortices at low temperatures”, Phys. Fluids **20**, 055105 (2008).
- [25] A. Golov and H. Ishimoto, “Sharp and Stable Metal Tips for Helium Ionization at mK Temperatures”, J. Low Temp. Phys. **113**, 957 (1998).
- [26] P. Hendry and P. V. E. McClintock, “Continuous flow apparatus for preparing isotopically pure He”, Cryogenics **27**, 131 (1987).
- [27] P. Hendry and P. V. E. McClintock, “ $^3\text{He}/^4\text{He}$ isotopic ratio measurements to below then 10^{-12} level”, Proceedings of LT-17 (1984).
- [28] P. V. E. McClintock, private communication, Feb. 6, 2022.
- [29] Boston Piezo-Optics, <https://www.bostonpiezooptics.com/>
- [30] D. Jin and H. Maris, “A Study of the Motion of Particles in Superfluid Helium-4 and Interactions with Vortices”, J. Low Temp. Phys. **162**, 329 (2011).
- [31] P. Meichle and D. P. Lathrop, “Nanoparticle dispersion in superfluid helium”, Rev. Sci. Instr. **85**, 073705 (2014).